Chemical Science

ROYAL SOCIETY OF CHEMISTRY

EDGE ARTICLE

View Article Online
View Journal | View Issue

Open Access Article. Published on 16 October 2025. Downloaded on 1/18/2026 3:43:07 AM.
This article is licensed under a Creative Commons Attribution-NonCommercial 3.0 Unported Licence.

Check for updates

Cite this: *Chem. Sci.*, 2025, **16**, 22536

All publication charges for this article have been paid for by the Royal Society of Chemistry

Received 3rd August 2025
Accepted 15th October 2025

DOI: 10.1039/d5sc05865a

rsc.li/chemical-science

Sequential oxidative dearomatization/asymmetric homologation: from simple naphthols to chiral benzocycloheptanes

Hongkun Zeng, Shiyang Li, Lichao Ning, Tao Huang, Xiaoming Feng * and Lili Lin *

An oxidative dearomatization/asymmetric ring-expansion sequential approach is reported to synthesize chiral benzocycloheptanes from unfunctionalized simple β-naphthols under mild reaction conditions. This protocol integrates a copper-catalyzed oxidative dearomatization of β-naphthols, following a chiral *N,N′*-dioxide-Sc(III) complex-promoted enantioselective homologation with α-diazoesters in one pot, enriching the chemistry of naphthol dearomatization. Computational studies demonstrate the process of Lewis acid-promoted homologation, as well as the origin of stereoselectivity.

Introduction

Chiral benzocycloheptanes, characterized by the fusion of one or two benzene rings with a seven-membered ring, constitute a pivotal structural motif in numerous pharmaceuticals and bioactive natural products.[1] For example, as dibenzocycloheptane-type compounds, allocolchicine functions as a tubulin-binding agent with potent activity against a broad spectrum of cancer cell lines;[2] dihyisosubamol demonstrates inhibitory activity against α-glucosidase type IV from *Bacillus stearothermophilus* (Scheme 1a).[3] Meanwhile, as mono-benzocycloheptane-type compounds, (*R*)-*ar*-himachalene functions as a male-specific aggregation pheromone, serving as a vital scientific tool for monitoring and managing economically important insect pests;[4] Hamigeran G exhibits potent anticancer and antitumor properties (Scheme 1b).[5] While numerous synthetic strategies for benzocycloheptane have been developed,[6] reports focusing on asymmetric catalysis remain remarkably scarce. In 2021, Ramasastry's group reported a chiral phosphine-catalyzed intramolecular asymmetric Morita–Baylis–Hillman reaction of enone-aldehydes, enabling the construction of dibenzocycloheptanes with moderate enantioselectivities.[7] In 2023, Chauhan and coworkers reported a bifunctional squaramide-catalyzed domino Michael/nitroaldol reaction between enone-aldehydes with β-keto compounds,[8] achieving chiral dibenzocycloheptanes in high efficiency (Scheme 1a). In 2025, Douglas disclosed an enantioselective transient directing group-mediated intramolecular hydroacylation approach to access chiral benzosuberones, enabled by cooperative Rh- and chiral 2-aminopyridine catalysis (Scheme 1b).[9] Developing other efficient protocols for the synthesis of chiral benzocycloheptanes, especially starting from simple feedstocks, holds significant merit.

Naphthols are important chemical materials and synthetic intermediates.[10] The oxidative dearomatization of naphthols efficiently furnishes benzocyclic carbonyl compounds.[11] On the other hand, diazo compounds serve as versatile synthons for one-carbon chain extension of carbonyl compounds *via* homologation reactions.[12] This process involves nucleophilic addition of the diazomethine carbon to the carbonyl carbon, followed by a 1,2-shift with nitrogen extrusion, enabling chain or ring expansion. We envisioned that *in situ* generation of 1,2-naphthoquinone from β-naphthol *via* oxidative dearomatization,[13] followed by an asymmetric ring-expansion reaction with an α-diazoester catalyzed by a chiral Lewis acid, would furnish a novel approach to benzocycloheptane construction. The challenges inherent to this strategy are twofold: (1) the oxidant or redox byproducts might interfere with the subsequent asymmetric homologation reaction; (2) the Lewis acid catalyst could promote decomposition of the in situ-generated naphthoquinone. Notwithstanding these hurdles, this tandem strategy holds promise as an efficient approach to constructing chiral benzocycloheptanes from simple starting materials.

Herein, we report the development of a Cu(I)/Sc(III) bimetallic catalytic system[14] that efficiently promotes the sequential[15] oxidative dearomatization/asymmetric homologation reaction of unfunctionalized β-naphthols with α-diazoesters, thereby enabling a novel strategy for the asymmetric synthesis of benzocycloheptanes (Scheme 1c).

Results and discussion

We initiated our investigation by employing β-naphthol **A1** and α-diazoester **B1** as model substrates to optimize the reaction

Key Laboratory of Green Chemistry & Technology, Ministry of Education, College of Chemistry, Sichuan University, Chengdu 610064, China. E-mail: xmfeng@scu.edu.cn; lililin@scu.edu.cn

© 2025 The Author(s). Published by the Royal Society of Chemistry

Open Access Article. Published on 16 October 2025. Downloaded on 1/18/2026 3:43:07 AM.
This article is licensed under a Creative Commons Attribution-NonCommercial 3.0 Unported Licence.

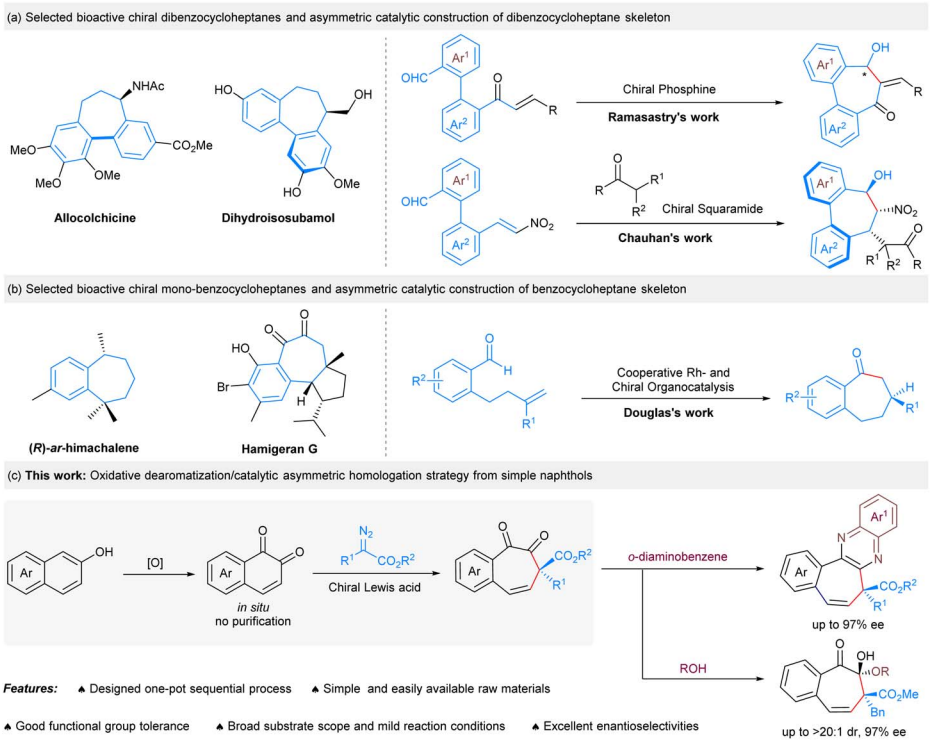

Scheme 1 Strategies for the synthesis of chiral benzocycloheptanes.

conditions. Following the catalytic reaction, *o*-diaminobenzene was introduced in a one-pot procedure to form quinoxaline **C1**, which is stable and facilitates chromatographic analysis (Table 1). Firstly, different oxidants were evaluated. No oxidative dearomatization product **D1** was observed when Oxone or TEMPO was used as the oxidant (entries 1 and 2). While IBX enabled the formation of **D1**, the subsequent homologation reaction was completely inhibited with $\mathbf{L_3}$-$\mathbf{TqPr_2}$/Sc(OTf)$_3$ as the chiral Lewis acid catalyst (entry 3). This inhibition is presumably due to the *in situ* generation of 2-iodobenzoic acid during the oxidation process, which may exert a detrimental effect on the catalyst activity. Gratifyingly, the combined CuBr/TBHP oxidation system not only afforded **D1** efficiently but also furnished the desired product **C1** in 38% yield with 81% ee (entry 4). The screening of copper salts revealed that CuCl outperformed both CuBr and $CuCl_2$ in terms of reaction yield (entries 5 and 6). According to the ^{1}H NMR analysis, the yield of **D1** was quantified to be 84%.

Subsequently, the reaction parameters for the asymmetric homologation were systematically explored. First, a range of metal salts in combination with $\mathbf{L_3}$-$\mathbf{TqPr_2}$ were screened. While Sc(OTf)$_3$ emerged as the optimal Lewis acid catalyst, other metal salts such as Cu(OTf)$_2$, Ln(OTf)$_3$, and Al(OTf)$_3$ failed to promote the reaction (entry 7). Next, the structural effects of the chiral *N*,*N*′-dioxide ligand were investigated. The results indicated that L-ramipril-derived $\mathbf{L_3}$-$\mathbf{RaPr_2}$ provided superior enantioselectivity compared to other amino acid-derived ligands, though the yield remained low (entries 8–10). Fine-tuning the linker length between the two N-oxide units revealed that a shorter linker not only enhanced the reaction efficiency but also maintained high enantioselectivity (entry 11, 42% yield, 96% ee). Control experiments confirmed that in the absence of a ligand, 1,2-naphthoquinone **D1** rapidly decomposed under Sc(OTf)$_3$ catalysis, and no desired product **C1** was detected;[16] whereas the homologation reaction did not occur in the absence of Sc(OTf)$_3$ (entries 12 and 13). Solvent screening further revealed that switching from DCE to DCM significantly improved the yield (entry 14, 57% yield, 97% ee). Despite extensive optimization efforts, further enhancement of the reaction yield remained elusive due to the inherent instability of **D1** under the reaction conditions and competing side reactions involving 1,2-carbonyl migration. Ultimately, the optimal conditions were established using CuCl/TBHP as the oxidant for oxidative dearomatization, Sc(OTf)$_3$/$\mathbf{L_2}$-$\mathbf{RaPr_2}$ as the Lewis acid catalyst for asymmetric homologation, and 1.2 equiv. of **B1** in DCM at 30 °C.

With the optimized conditions established, the substrate scope was explored (Scheme 2). For benzyl diazoesters, variations in electronic properties had minimal impact on reaction efficiency and enantioselectivity. Both electron-donating groups (*e.g.*, Me, ^{t}Bu, Ph, OMe, and SMe) and electron-withdrawing substituents (*e.g.*, halogen, CO_2Me, OCF_3, and SCF_3) at the *para*-position of the phenyl ring furnished the products **C1–C13** in 32–57% yields with 93–97% ee. The 3-methylbenzyl derivative **B14** afforded **C14** in 50% yield and 95% ee, whereas the 2-methylbenzyl analogue **B15** exhibited significantly reduced reactivity, presumably due to steric hindrance during the reaction. Fused-ring and heterocyclic diazoesters also provided the desired seven-membered ring products with moderate yields

Open Access Article. Published on 16 October 2025. Downloaded on 1/18/2026 3:43:07 AM.
This article is licensed under a Creative Commons Attribution-NonCommercial 3.0 Unported Licence.

Table 1 Optimization of the reaction conditions[a]

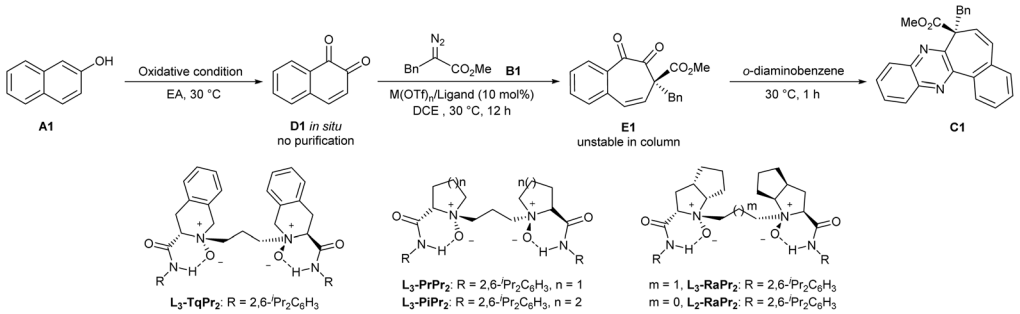

Entry	Oxidative condition	M^{n+}	Ligand	Yield of **C1**[b] (%)	Ee of **C1**[c] (%)
1	Oxone	$Sc(OTf)_3$	**L_3-TqPr$_2$**	N.R.	—
2	TEMPO	$Sc(OTf)_3$	**L_3-TqPr$_2$**	N.R.	—
3	IBX	$Sc(OTf)_3$	**L_3-TqPr$_2$**	0	—
4[d]	CuBr/TBHP	$Sc(OTf)_3$	**L_3-TqPr$_2$**	38	81
5[d]	CuCl/TBHP	$Sc(OTf)_3$	**L_3-TqPr$_2$**	50	83
6[d]	$CuCl_2$/TBHP	$Sc(OTf)_3$	**L_3-TqPr$_2$**	43	81
7[d]	CuCl/TBHP	Cu^{2+}, Ln^{3+}, Al^{3+}…	**L_3-TqPr$_2$**	0	—
8[d]	CuCl/TBHP	$Sc(OTf)_3$	**L_3-RaPr$_2$**	31	95
9[d]	CuCl/TBHP	$Sc(OTf)_3$	**L_3-PrPr$_2$**	28	80
10[d]	CuCl/TBHP	$Sc(OTf)_3$	**L_3-PiPr$_2$**	48	80
11[d]	CuCl/TBHP	$Sc(OTf)_3$	**L_2-RaPr$_2$**	42	96
12[d]	CuCl/TBHP	$Sc(OTf)_3$	—	0	—
13[d]	CuCl/TBHP	—	**L_2-RaPr$_2$**	0	—
14[d,e]	CuCl/TBHP	$Sc(OTf)_3$	**L_2-RaPr$_2$**	57	97

[a] Reaction conditions: β-naphthol **A1** (0.1 mmol), oxidant (0.1 mmol), EA (1.0 mL), 30 °C, 16 h; then ligand/$M(OTf)_n$ (1 : 1, 10 mol%), α-diazoester **B1** (0.12 mmol), DCE (1.0 mL), 30 °C, 12 h; then *o*-diaminobenzene (1.5 equiv.), 30 °C, 1 h. [b] Yields of isolated products. [c] Ee was determined by UPC[2] analysis on a chiral stationary phase. [d] [Cu] (10 mol%), TBHP (4.0 equiv.), 2 h. [e] DCM instead of DCE. Oxone = potassium monopersulphate triple salt. TBHP = *tert*-butyl hydroperoxide. IBX = 2-iodoxybenzoic acid. TEMPO = 2,2,6,6-tetramethylpiperidinooxy. N.R. = no reaction.

and excellent ee (**C16–C18**, 52–58% yield, 94–96% ee). Linear extension of the benzyl chain (**B19–B20**) maintained high enantioselectivity (95% and 91% ee, respectively). Substitution with a cinnamyl moiety was also suitable, and **C21** was obtained in 52% yield with 95% ee. Terpene-derived diazoesters **B22–B23** reacted smoothly, and notably, *n*-octadecane-derived diazoester **B24** was also compatible, providing the corresponding product in 50% yield and 90% ee. Evaluation of ester substituents (**B25–B29**) revealed that bulky groups (*e.g.*, cyclopentyl, 2-ethylbutyl, cyclopropylmethyl, cyclopentylmethyl, and cyclohexylmethyl) had little effect on the enantioselectivity (**C25–C29**, 42–52% yield, 92–94% ee).

Next, the scope of β-naphthols was explored. β-Naphthols bearing various functional groups at the C6-position were found compatible with the reaction conditions, smoothly furnishing the corresponding products (**C30–C35**, 92–98% ee). Generally, substrates containing electron-donating groups (*e.g.*, Et, Ph, and OMe) provided higher yields than those with electron-withdrawing groups (*e.g.*, Br, CO_2Me, and CN). The 6-styryl substituted substrate **B36** afforded product **C36** in 38% yield with excellent enantioselectivity. Additionally, C7-functionalized substrates underwent the reaction efficiently, yielding the target compounds in moderate yields with outstanding ee values (**C37–C39**, 50–59% yield, 94–97% ee). The absolute configuration of product **C4** was unambiguously determined to be (*S*) by X-ray crystallographic analysis.[17]

The use of unsymmetric *o*-diaminobenzene resulted in the formation of two regioisomers. For instance, 4-methyl-1,2-phenylenediamine furnished an inseparable **C40**/**C40′** regioisomer mixture (combined yield: 60%, 97%/96% ee, rr = 46 : 54). C4-position substitution with an electron-withdrawing Cl group was tolerated, albeit with reduced reactivity (**C41**/**C41′**: 19%/23% yield, 97%/91% ee, rr = 45 : 55). Additionally, C2-position substituents—whether electron-donating (Me) or electron-withdrawing (Cl)—delivered target products in moderate yields: **C42**/**C42′** (20%/30% yield, 97%/91% ee, rr = 40 : 60) and **C43**/**C43′** (27%/21% yield, 97%/87% ee, rr = 56 : 44).

Upon treatment with alcohols in place of *o*-phenylenediamine following the homologation reaction, hemiketal compounds could be obtained in moderate yields with excellent stereoselectivity (Scheme 3, **F1–F3**, 42–45% yield, 97% ee, >20 : 1 dr).

To demonstrate the synthetic utility of this methodology, a scaled-up synthesis and functional group transformations of compound **C1** were conducted. Under optimized conditions, β-naphthol **A1** (5.0 mmol) reacted smoothly with α-

 © 2025 The Author(s). Published by the Royal Society of Chemistry

Open Access Article. Published on 16 October 2025. Downloaded on 1/18/2026 3:43:07 AM.
This article is licensed under a Creative Commons Attribution-NonCommercial 3.0 Unported Licence.

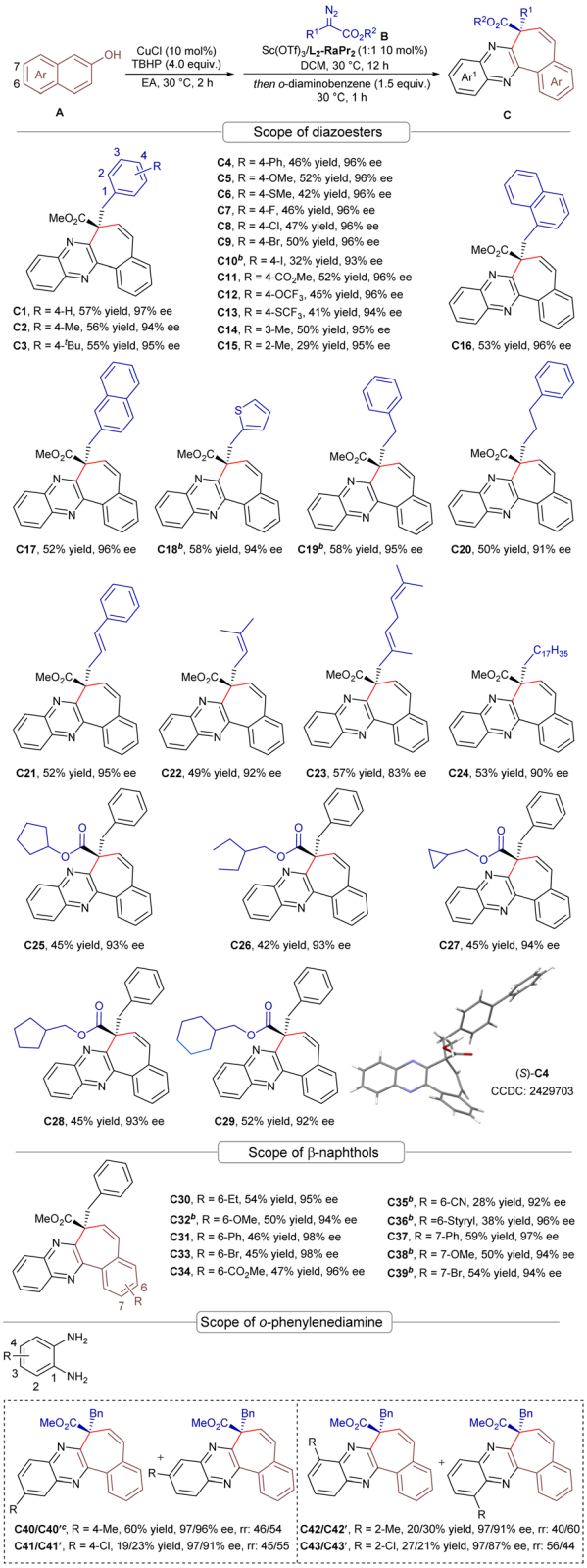

Scheme 2 Substrate scope.[a] [a]Reaction conditions: β-naphthol **A** (0.1 mmol), CuCl (10 mol%) and TBHP (4.0 equiv.) in EA (1.0 mL) at 30 °C for 2 h; then **L₂-RaPr₂**/Sc(OTf)$_3$ (1 : 1, 10 mol%) and α-diazoester **B** (0.12 mmol) in DCM (1.0 mL) at 30 °C for 12 h; then *o*-diaminobenzene (0.15 mmol) at 30 °C for 1 h. Isolated yield. Ee was determined by HPLC or UPC^2 on a chiral stationary phase. [b]**L₂-RaPr₂**/Sc(OTf)$_3$ (1 : 1, 10 mol%) and α-diazoester **B** (0.12 mmol) in DCM (1.0 mL) at 30 °C for 24 h. [c]Isolated as a mixture of regiosomers.

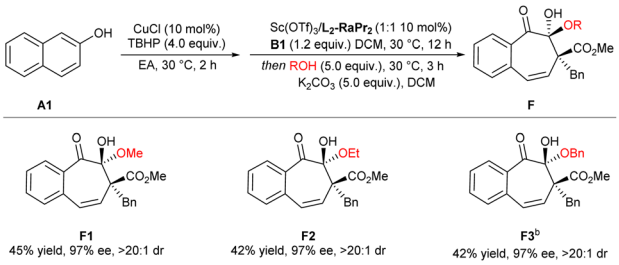

Scheme 3 Synthesis of chiral hemiketal compounds.[a] [a]Reaction conditions: **A1** (0.1 mmol), CuCl (10 mol%) and TBHP (4.0 equiv.) in EA (1.0 mL) at 30 °C for 2 h; then **L₂-RaPr₂**/Sc(OTf)$_3$ (1 : 1, 10 mol%) and **B1** (0.12 mmol) in DCM (1.0 mL) at 30 °C for 12 h; then ROH (0.5 mmol) and K_2CO_3 (0.5 mmol) at 30 °C for 3 h. Isolated yield. Ee was determined by UPC^2 on a chiral stationary phase. Dr was determined by ^{1}H NMR. [b] ROH (0.5 mmol) and K_2CO_3 (0.5 mmol) at 30 °C for 5 h.

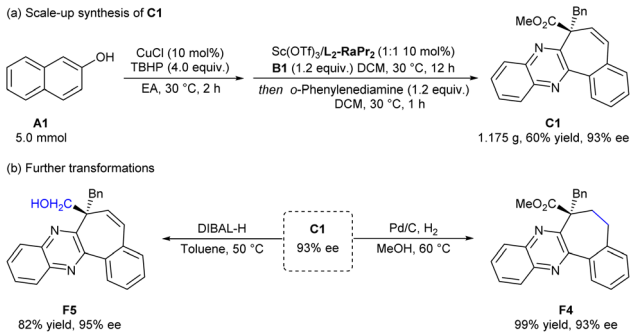

Scheme 4 (a) Scale-up synthesis of **C1**; (b) further transformations.

diazoester **B1**, furnishing product **C1** in 60% yield with 93% ee (Scheme 4a). Subsequent reduction of **C1** with Pd/C in MeOH at 60 °C effectively hydrogenated the C=C bond, yielding compound **F4** in 99% yield. The methoxycarbonyl group was selectively reduced by DIBAL-H in toluene at 50 °C, affording alcohol **F5** in 82% yield. Notably, there was no loss of optical purity in the products throughout these transformations (Scheme 4b).

The reaction mechanism of the Lewis acid-promoted homologation was analyzed through a detailed computational study, as depicted in the reaction energy profile (Scheme 5). The catalytic process initiates with the formation of intermediate **INT1**, wherein the Sc(III)/**L₂-RaPr₂** complex coordinates to **D1** in a bidentate manner,[18] generating the initial complex **INT1**. Subsequently, the alkyl diazoester **B1** initiates a nucleophilic attack on the more electropositive carbonyl carbon of **D1**, leading to the formation of intermediate **INT2** *via* transition state **TS1**. The energy barrier for the formation of the *S*-configured product (**TS1-*S***) in this process is 1.3 kcal mol^{-1} lower than that for the formation of the *R*-configured product (**TS1-*R***). Structure analysis reveals that in **TS1-*S***, there is a CH–π interaction between the phenyl group in **B1** and the phenyl group of the ligand. Subsequently, the ring-expansion reaction occurs *via* transition state **TS2**, featuring a relatively low activation barrier of 3.3 kcal mol^{-1}, ultimately releasing the product and regenerating the catalyst.

Open Access Article. Published on 16 October 2025. Downloaded on 1/18/2026 3:43:07 AM.
This article is licensed under a Creative Commons Attribution-NonCommercial 3.0 Unported Licence.

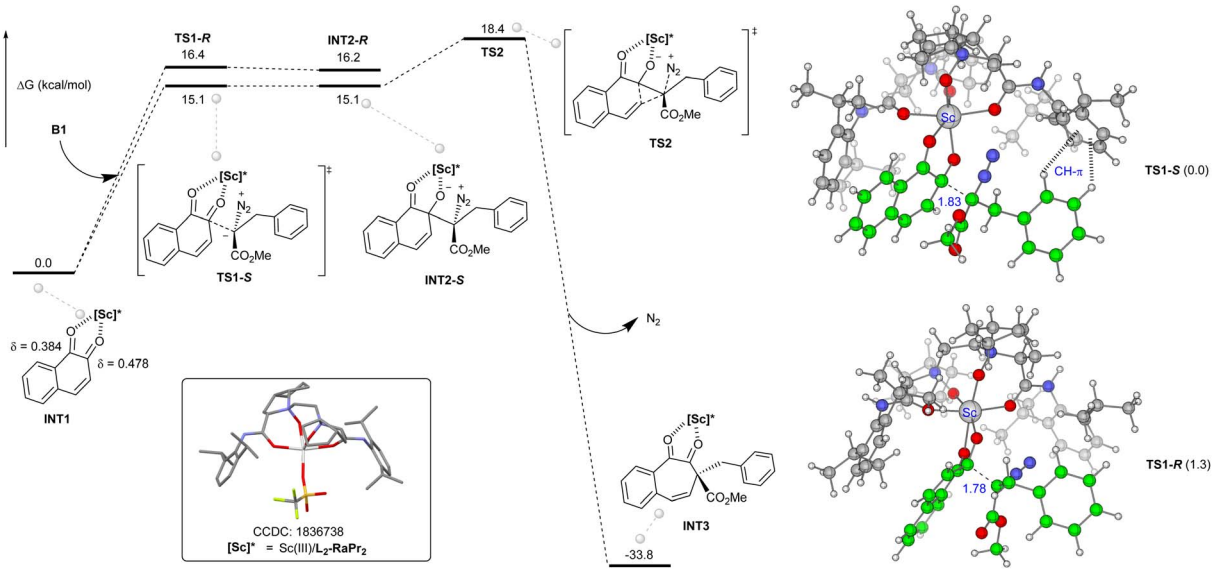

Scheme 5 DFT-calculated Gibbs free energy profile for the asymmetric homologation step, showing structures and relative Gibbs free energies of TS1-*S* and TS1-*R*.

Conclusions

In summary, we have successfully developed an efficient oxidative dearomatization/asymmetric homologation reaction for non-functionalized β-naphthols. This methodology integrates a copper-catalyzed oxidative dearomatization reaction of β-naphthols with a chiral *N*,*N*′-dioxide-Sc^{III} complex-promoted enantioselective homologation reaction of α-diazoesters in a one-pot procedure. A series of valuable optically active benzocycloheptane derivatives were synthesized in moderate to good yields with excellent ee values. The synthetic utility is further validated by scale-up synthesis and post-reaction functional group transformations. Notably, this stepwise strategy enriched the chemistry of naphthol desymmetrization.

Data availability

CCDC 2429703 (**C4**) contains the supplementary crystallographic data for this paper.[19]

Supplementary information: ^{1}H, $^{13}C\{^{1}H\}$ and $^{19}F\{^{1}H\}$ NMR, HPLC and UPC[2] spectra (PDF). See DOI: **https://doi.org/10.1039/d5sc05865a**.

Author contributions

H. K. Z. performed the experiments. L. C. N. conducted the DFT calculation. S. Y. L. participated in the synthesis of substrates. T. H. repeated the experiments to validate the data. X. M. F and L. L. L. supervised the project. H. K. Z. and L. L. L. co-wrote the manuscript.

Conflicts of interest

There are no conflicts to declare.

Acknowledgements

We appreciate the National Key R&D Program of China (2023YFA1506700) and the National Natural Science Foundation of China (No. 22171189) for financial support. We are grateful to Dr Yuqiao Zhou from the College of Chemistry, Sichuan University, for the X-ray single crystal diffraction analysis.

Notes and references

1 (*a*) J.-H. Fan, Y.-J. Hu, L.-X. Li, J.-J. Wang, S.-P. Li, J. Zhao and C.-C. Li, *Nat. Prod. Rep.*, 2021, **38**, 1821–1851; (*b*) M. Leblanc and K. Fagnou, *Org. Lett.*, 2005, **7**, 2849–2852; (*c*) K. C. Nicolaou, T. R. Wu, Q. Kang and D. Y.-K. Chen, *Angew. Chem., Int. Ed.*, 2009, **48**, 3440–3443; (*d*) K. C. Nicolaou, Q. Kang, T. R. Wu, C. S. Lim and D. Y.-K. Chen, *J. Am. Chem. Soc.*, 2010, **132**, 7540–7548; (*e*) S. A. Snyder, T. C. Sherwood and A. G. Ross, *Angew. Chem., Int. Ed.*, 2010, **49**, 5146–5150; (*f*) J. Li, P. Yang, M. Yao, J. Deng and A. Li, *J. Am. Chem. Soc.*, 2014, **136**, 16477–16480; (*g*) D. J. Paymode and C. V. Ramana, *ACS Omega*, 2017, **2**, 5591–5600; (*h*) S. S. Goh, G. Chaubet, B. Gockel, M. Caroline, A. Cordonnier, H. Baars, A. W. Phillips and E. A. Anderson, *Angew. Chem., Int. Ed.*, 2015, **54**, 12618–12621.
2 (*a*) G. Micheletti, M. Poli, P. Borsotti, M. Martinelli, B. Imberti, G. Taraboletti and R. Giavazzi, *Cancer Res.*, 2003, **63**, 1534; (*b*) T. Graening and H. G. Schmalz, *Angew. Chem., Int. Ed.*, 2004, **43**, 3230–3256.
3 H.-C. Lin and S.-S. Lee, *J. Nat. Prod.*, 2012, **75**, 1735–1743.
4 S. P. Chavan and H. S. Khatod, *Tetrahedron: Asymmetry*, 2012, **23**, 1410–1415.
5 E. F. Woolly, A. J. Singh, E. R. Russell, J. H. Miller and P. T. Northcote, *J. Nat. Prod.*, 2018, **81**, 387–393.

 © 2025 The Author(s). Published by the Royal Society of Chemistry

Open Access Article. Published on 16 October 2025. Downloaded on 1/18/2026 3:43:07 AM.
This article is licensed under a Creative Commons Attribution-NonCommercial 3.0 Unported Licence.

6 (*a*) L. F. Silva Jr, R. S. Vasconcelos and M. A. Nogueira, *Org. Lett.*, 2008, **10**, 1017–1020; (*b*) U. K. Tambar and B. M. Stoltz, *J. Am. Chem. Soc.*, 2005, **127**, 5340–5341; (*c*) S. B. L. Silva, A. D. Torre, J. E. de Carvalho, A. L. T. G. Ruiz and L. F. Silva Jr, *Molecules*, 2015, **20**, 1475–1494; (*d*) Y. Xia, S. Ochi and G. B. Dong, *J. Am. Chem. Soc.*, 2019, **141**, 13038–13042; (*e*) Q. Y. Yao, L. K. Kong, M. D. Wang, Y. Yuan, R. Z. Sun and Y. Z. Li, *Org. Lett.*, 2018, **20**, 1744–1747; (*f*) H. Okawa, T. Kawasaki-Takasuka and K. Mori, *Org. Lett.*, 2024, **26**, 1662–1666; (*g*) Y. Otawa and K. Mori, *Chem. Commun.*, 2019, **55**, 13856–13859; (*h*) M. Kataoka, Y. Otawa, N. Ido and K. Mori, *Org. Lett.*, 2019, **21**, 9334–9338; (*i*) F. Bodinier, Y. Sanogo, J. Ardisson, M.-I. Lannou and G. Sorin, *Chem. Commun.*, 2021, **57**, 3603–3606; (*j*) D. Pflästerer, E. Rettenmeier, S. Schneider, E. de Las Heras Ruiz, M. Rudolph and A. S. K. Hashmi, *Chem.–Eur. J.*, 2014, **20**, 6752–6755; (*k*) B. Kramer and S. R. Waldvogel, *Angew. Chem., Int. Ed.*, 2004, **43**, 2446–2449; (*l*) K. Hackeloer, G. Schnakenburg and S. R. Waldvogel, *Org. Lett.*, 2011, **13**, 916–919; (*m*) W. Q. Kong, N. Fuentes, A. G. Domínguez, E. Merino and C. Nevado, *Angew. Chem., Int. Ed.*, 2015, **54**, 2487–2491; (*n*) Z. M. Xing, B. W. Fang, S. W. Luo, X. G. Xie and X. L. Wang, *Org. Lett.*, 2022, **24**, 4034–4039; (*o*) T. Kikuchi, K. Yamada, T. Yasui and Y. Yamamoto, *Org. Lett.*, 2021, **23**, 4710–4714.

7 A. M. Shivangi, P. Tung, S. V. Wagulde and S. S. V. Ramasastry, *Chem. Commun.*, 2021, **57**, 9260–9263.

8 N. Kotwal, Tamanna, A. Changotra and P. Chauhan, *Org. Lett.*, 2023, **25**, 7523–7528.

9 P. B. Staub, H. M. Holst, N. N. Puthalath and C. J. Douglas, *ACS Catal.*, 2025, **15**, 11512–11518.

10 (*a*) M. Weber, M. Weber and M. Kleine-Boymann, Phenol, in *Ullmann's Encyclopedia of Industrial Chemistry*, Wiley-VCH, Weinheim, Germany, 2004, vol. 56, p. 503; (*b*) F. Visioli, A. Poli and C. Galli, *Med. Res. Rev.*, 2002, **22**, 65–75.

11 (*a*) C.-X. Zhuo, W. Zhang and S.-L. You, *Angew. Chem., Int. Ed.*, 2012, **51**, 12662–12686; (*b*) R. Kumar, F. V. Singh, N. Takenaga and T. Dohi, *Chem.–Asian J.*, 2022, **17**, e202101115; (*c*) H. Y. Zhang, N. Xu, R. P. Tang and X. L. Shi, *Chin. J. Org. Chem.*, 2023, **43**, 3784–3805; (*d*) M. F. McLaughlin, E. Massolo, S. B. Liu and J. S. Johnson, *J. Am. Chem. Soc.*, 2019, **141**, 2645–2651.

12 For the reviews, see: (*a*) M. P. Doyle, M. A. McKervey and T. Ye, *Modern Catalytic Methods for Organic Synthesis with Diazo Compounds*, Wiley, New York, 1998; (*b*) Y. Zhang and J. B. Wang, *Chem. Commun.*, 2009, **36**, 5350–5361; (*c*) N. R. Candeias, R. Paterna and P. M. P. Gois, *Chem. Rev.*, 2016, **116**, 2937–2981; (*d*) S. X. Dong, X. H. Liu and X. M. Feng, *Acc. Chem. Res.*, 2022, **55**, 415–428, For the selected examples of homologation reactions, see: ; (*e*) T. Hashimoto, Y. Naganawa and K. Maruoka, *J. Am. Chem. Soc.*, 2011, **133**, 8834–8837; (*f*) V. L. Rendina, D. C. Moebius and J. S. Kingsbury, *Org. Lett.*, 2011, **13**, 2004–2007; (*g*) W. Li, X. H. Liu, X. Y. Hao, Y. F. Cai, L. L. Lin and X. M. Feng, *Angew. Chem., Int. Ed.*, 2012, **51**, 8644–8647; (*h*) W. Li, F. Tan, X. Y. Hao, G. Wang, Y. Tang, X. H. Liu, L. L. Lin and X. M. Feng, *Angew. Chem., Int. Ed.*, 2015, **54**, 1608–1611; (*i*) W. Li, X. H. Liu, F. Tan, X. Y. Hao, J. F. Zheng, L. L. Lin and X. M. Feng, *Angew. Chem., Int. Ed.*, 2013, **52**, 10883–10886; (*j*) X. F. Li, P. P. He, P. Zhu, Y. H. Tang and Y. G. Peng, *Org. Chem. Front.*, 2023, **10**, 1564–1569; (*k*) S.-S. Li, S. Sun and J. B. Wang, *Angew. Chem., Int. Ed.*, 2022, **61**, e202115098; (*l*) H.-M. Jeong, J. W. Lee, D. K. Kim and D. H. Ryu, *ACS Catal.*, 2024, **14**, 131–137; (*m*) S. Y. Li, C. F. Zhang, G. H. Pan, L. K. Yang, Z. S. Su, X. M. Feng and X. H. Liu, *ACS Catal.*, 2023, **13**, 4656–4666.

13 (*a*) M. Uyanik, T. Mutsuga and K. Ishihara, *Molecules*, 2012, **17**, 8604–8616; (*b*) J. Sim, H. Jo, M. Viji, M. Choi, J.-A. Jung, H. Lee and J.-K. Jung, *Adv. Synth. Catal.*, 2018, **360**, 852–858; (*c*) A. K. Mishra and J. N. Moorthy, *J. Org. Chem.*, 2016, **81**, 6472–6480; (*d*) A. H. Wu, Y. Z. Duan, D. W. Xu, T. M. Penning and R. G. Harvey, *Tetrahedron*, 2010, **66**, 2111–2118.

14 (*a*) D. R. Pyea and N. P. Mankad, *Chem. Sci.*, 2017, **8**, 1705–1718; (*b*) J. Xu, G. Y. Wang, K. L. Ding and X. M. Wang, *J. Am. Chem. Soc.*, 2025, **147**, 2000–2009; (*c*) Z.-J. Jia, G. Shan, C. G. Daniliuc, A. P. Antonchick and H. Waldmann, *Angew. Chem., Int. Ed.*, 2018, **57**, 14493–14497; (*d*) H. X. Huo, G. L. Li, X. Wang and W. B. Zhang, *Angew. Chem., Int. Ed.*, 2022, **61**, e202210086; (*e*) X. P. Sang, W. T. Xu, Y. Q. Zhou, M. Chen, L. L. Lin, M. H. Ji, F. Wang, S. X. Dong and X. M. Feng, *Sci. China: Chem.*, 2025, **68**, 5007–5015.

15 (*a*) Q.-J. Liang, Y.-H. Xu and T.-P. Loh, *Org. Chem. Front.*, 2018, **5**, 2765–2768; (*b*) Z. W. Wu, X. M. Feng and Y. B. Liu, *Synthesis*, 2024, **56**, 3349–3364.

16 S. X. Dong, W. D. Cao, M. P. Pu, X. H. Liu and X. M. Feng, *CCS Chem.*, 2023, **5**, 2717–2735.

17 CCDC munbers 2429703 (**C4**) contains the supplementary crystallographic data for this paper.

18 (*a*) F. Tan, M. P. Pu, J. He, J. Z. Li, J. Yang, S. X. Dong, X. H. Liu, Y. D. Wu and X. M. Feng, *J. Am. Chem. Soc.*, 2021, **143**, 2394–2402; (*b*) W. D. Cao, X. H. Liu and X. M. Feng, *Chin. Sci. Bull.*, 2020, **65**, 2941–2951; (*c*) H. K. Zeng, G. Weng, L. L. Lin and X. M. Feng, *Chem. Commun.*, 2024, **60**, 7507–7510; (*d*) J. Q. Tan, L. Q. Yang, H. Y. Su, Y. T. Yang, Z. W. Zhong, X. M. Feng and X. H. Liu, *Chem. Sci.*, 2024, **15**, 16050–16058; (*e*) L. L. Lin, Y. Q. Zhou, W. D. Cao, S. X. Dong, X. H. Liu and X. M. Feng, *Sci. Sin.: Chim.*, 2023, **53**, 246–258.

19 CCDC 2429703: Experimental Crystal Structure, 2025, DOI: **10.5517/ccdc.csd.cc2mk9j1**.